Electronic Supplementary Information

Hydrogen evolution reaction activity of nickel phosphide is highly sensitive to electrolyte pH

Zheng Zhou,[a] Li Wei,*[a] Yanqing Wang,[b] H. Enis Karahan,[c] Zibin Chen,[d] Yaojie Lei,[a] Xuncai Chen,[a] Shengli Zhai,[a,c] Xiaozhou Liao,[d] Yuan Chen*[a]

[a]The University of Sydney, School of Chemical and Biomolecular Engineering, Sydney, New South Wales, 2006, Australia E-mail: l.wei@sydney.edu.au; yuan.chen@sydney.edu.au

[b]The University of Tokyo, Faculty of Engineering, Yayoi, Bunkyo-ku, Tokyo, 113-0032 Japan

[c]Nanyang Technological University, School of Chemical and Biomedical Engineering, 637459, Singapore

[d]The University of Sydney, School of Aerospace, Mechanical & Mechatronic Engineering, Sydney, New South Wales, 2006, Australia

Preparation of Ni_2P electrodes

Ti foils (Sigma-Aldrich, 99.7%, 3 cm in length, 0.5 cm in width and 0.13 mm in thickness) were first cleaned by sonication in acetone and isopropanol solutions for 10 min, respectively. Next, Ni films were electrodeposited on the cleaned Ti foils in 1 M $NiSO_4$ electrolyte (pH adjusted to 2 using 1 M H_2SO_4) using an electrochemical workstation (CHI, 660D). The Ti foils were immerged in the electrolyte about 1 cm in depth. Carbon rods (99.999%, Strem Chemicals) as the counter electrode and a saturated calomel electrode (SCE) (in saturated KCl) were used as the counter and reference electrode, respectively. Chronoamperometry was applied at the cathodic current density of 10 $mA \cdot cm^{-2}$ for 900 s. Subsequently, Ni oxide layers were formed by dipping the Ni films in 0.1 M KOH solution under the potential of 1.1 V (*vs.* RHE) for 900 s. Afterwards, the Ni oxide layers were phosphorized to produce Ni_2P catalysts in a tube furnace. About 1.4 g of NaH_2PO_2 (Sigma-Aldrich) was loaded in a ceramic boat and placed at the upstream in the tube furnace to generate PH_3. Ti foils with Ni oxide layers were placed at the downstream approximately 5 cm away from NaH_2PO_2. The tube furnace was first purged with Ar (50 sscm) for 30 min, and then heated at 5 $^oC\ min^{-1}$ to 280 ^oC and held at the temperature for 1 h. After phosphorization, the furnace was cooled to room temperature under flowing Ar.

Preparation of electrolytes at different pH

Following the procedure developed in a previous study,[1] 19 electrolytes in the range from 0.52 to 13.53 were prepared. Among them, 11 electrolytes were pH-buffered from 2.71 to 10.46. First, sulphuric acid (H_2SO_4, 0.5 and 0.1 M), phosphoric acid (H_3PO_4, 0.1 M), acetate acid (CH_3COOH, 1 M and 0.3 M) and potassium hydroxide (KOH; 3.7 M, 1 M and 0.1 M) electrolytes were prepared by adding H_2SO_4 (Sigma-Aldrich, 98 wt%), H_3PO_4 (Sigma-Aldrich, 85 wt%), CH_3COOH (Sigma-Aldrich, ≥99 wt%) and KOH pellet (Sigma-Aldrich) into deionised (DI) water, respectively. Sodium acetate solution (CH_3COONa; 0.2M), sodium carbonate solution (Na_2CO_3, 0.2 M) and sodium bicarbonate solution ($NaHCO_3$, 0.2 M) were prepared by adding CH_3COONa (Sigma-Aldrich, ≥99 wt%), Na_2CO_3 (Sigma-Aldrich, ≥99 wt%) and $NaHCO_3$ (Sigma-Aldrich, ≥99 wt%) into DI water, respectively. Acetate buffer was prepared by

mixing different ratio of 0.3 M (or 1 M for pH < 3) CH_3COOH and 0.2 M CH_3COONa solutions; phosphoric buffer was prepared by adding different amount of 3.7 M KOH into 0.2 M H_3PO_4 solution; (bi)carbonate buffer was prepared by mixing different ratios of 0.2 M Na_2CO_3 and 0.2 M $NaHCO_3$ solutions.

Table S1. Composition of electrolytes at different pH

Electrolytes	**pH**	**Composition**
H_2SO_4	0.52	0.5 M H_2SO_4
H_2SO_4	1.10	0.1 M H_2SO_4
H_3PO_4	1.68	0.1 M H_3PO_4
H_3PO_4	2.81	0.1 M H_3PO_4 diluted
acetate buffer solution	2.71	1 M CH_3COOH (48.0 mL) + 0.2 M CH_3COONa (2.0 mL)
acetate buffer solution	3.54	0.3 M CH_3COOH (40.0 mL) + 0.2 M CH_3COONa (10.0 mL)
acetate buffer solution	4.48	0.3 M CH_3COOH (25.0 mL) + 0.2 M CH_3COONa (25.0 mL)
acetate buffer solution	5.39	0.3 M CH_3COOH (10.0 mL) + 0.2 M CH_3COONa (40.0 mL)
phosphoric buffer solution	5.40	0.2 M H_3PO_4 (40.0 mL) + 3.7 M KOH (2.7 mL)
phosphoric buffer solution	6.15	0.2 M H_3PO_4 (40.0 mL) + 3.7 M KOH (3.4 mL)
phosphoric buffer solution	7.21	0.2 M H_3PO_4 (40.0 mL) + 3.7 M KOH (4.6 mL)
phosphoric buffer solution	8.28	0.2 M H_3PO_4 (40.0 mL) + 3.7 M KOH (5.0 mL)
(bi)carbonate buffer solution	8.26	0.2 M $NaHCO_3$ (49.0 mL) + 0.2 M Na_2CO_3 (1.0 mL)
(bi)carbonate buffer solution	9.28	0.2 M $NaHCO_3$ (35.0 mL) + 0.2 M Na_2CO_3 (15.0 mL)
(bi)carbonate buffer solution	10.46	0.2 M $NaHCO_3$ (5.0 mL) + 0.2 M Na_2CO_3 (45.0 mL)
KOH	10.41	0.1 M KOH diluted
KOH	11.33	0.1 M KOH diluted
KOH	12.42	0.1 M KOH
KOH	13.53	1 M KOH

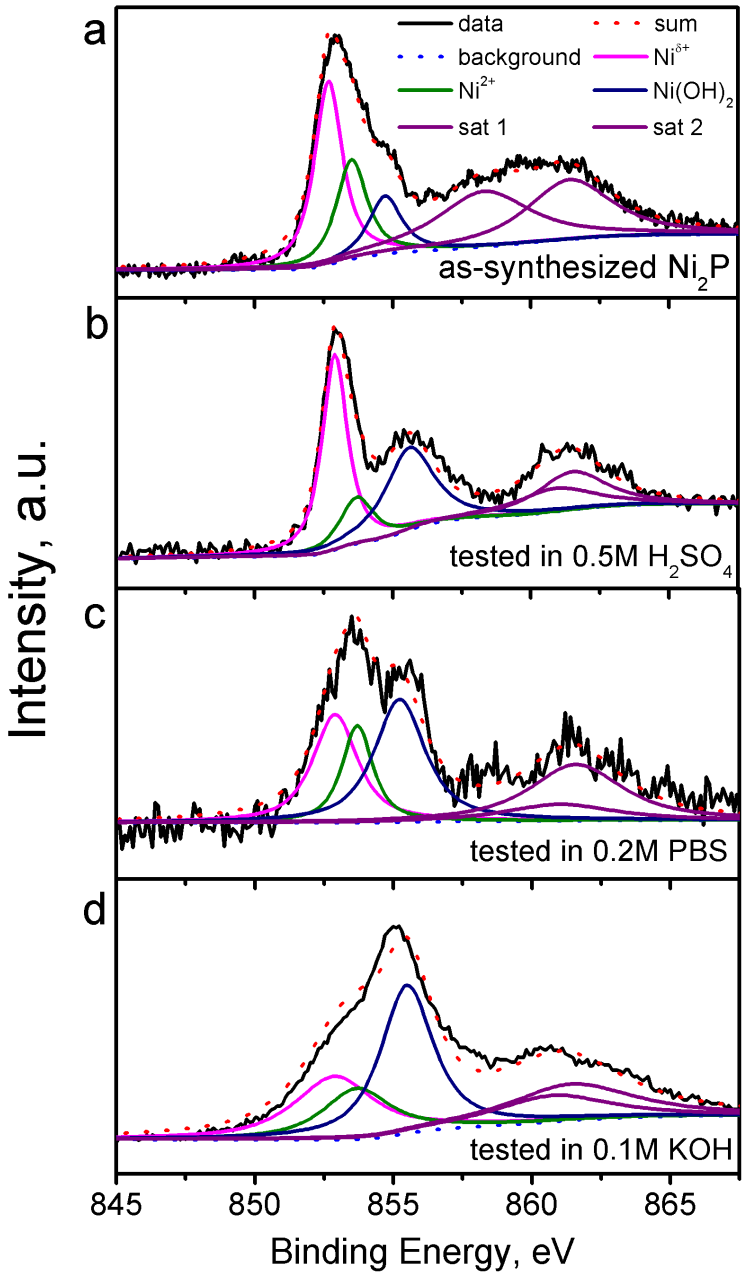

Fig. S1. High-resolution XPS spectra of Ni_2P electrodes (a) as synthesized, and (b-d) after HER tests in different electrolytes. (b) 0.5 M H_2SO_4, (c) 0.2 M phosphoric buffer, and (d) 0.1 M KOH.

Table S2. Surface composition of Ni_2P electrodes at different conditions: as synthesized and after HER test in different electrolytes. The ratio is calculated from the XPS peak area determined in Fig. S1.

	Ratio (at. %)		
Sample	$Ni^{\delta+}$	Ni^{2+}	$Ni(OH)_2$
As-synthesized	51.5	30.1	18.4
H_2SO_4	40.2	24.2	35.6
PBS	34.5	21.4	44.1
KOH	29.8	25.0	45.2

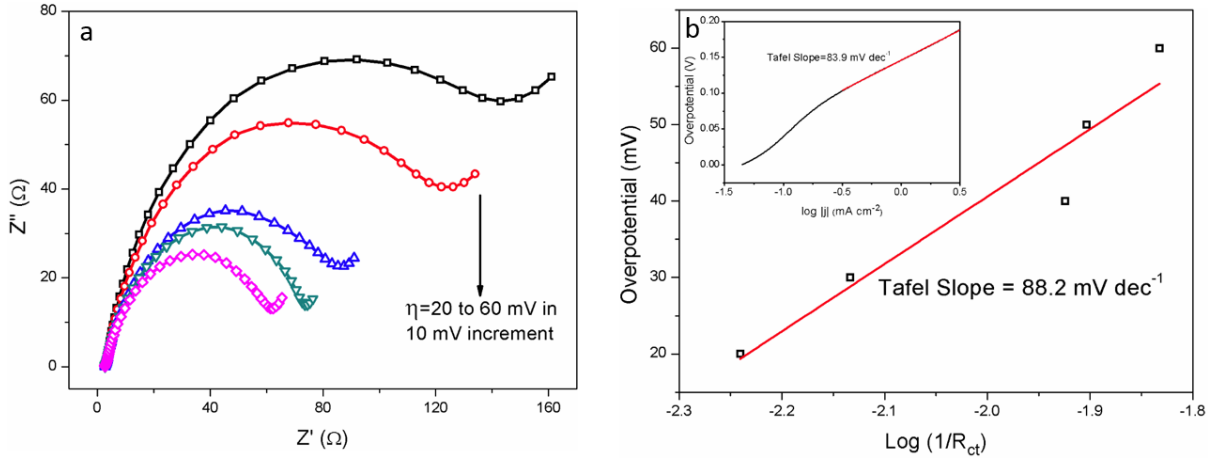

Fig. S2. (a) Nyquist plot and fitting results of the impedance response of the Ni_2P electrode, (b) Plot of $\log(R_{ct}^{-1})$ *vs.* η for the Ni_2P electrode. The insert is the Tafel plot obtained from the polarization curve. All measurements were performed in 0.5 M H_2SO_4.

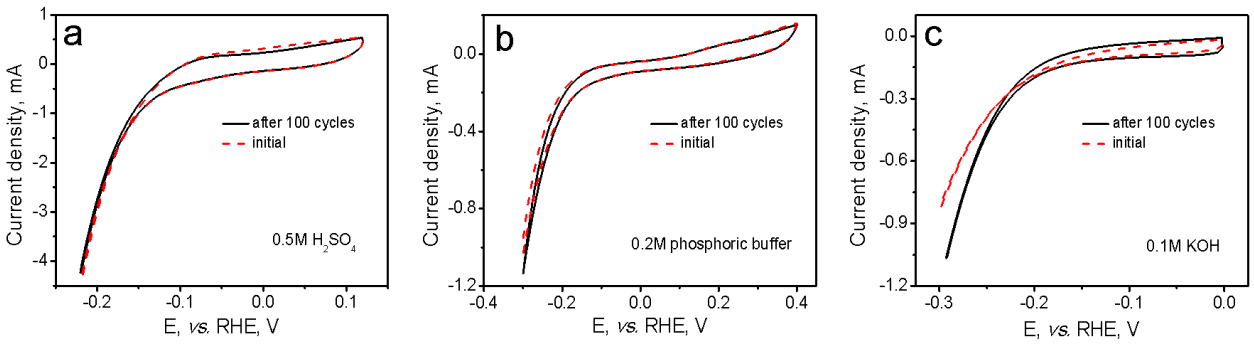

Fig. S3. CV curves of Ni_2P: (a) in 0.5 M H_2SO_4, (b) in 0.2 M phosphoric buffer, (c) in 0.1 M KOH.

Table S3. EDS element ratio before/after tested in 0.1 M KOH.

	Ratio (%)			
Sample	Ni	P	O	Ti
Before	60.0	25.1	14.1	0.8
After	76.7	13.3	8.3	1.7

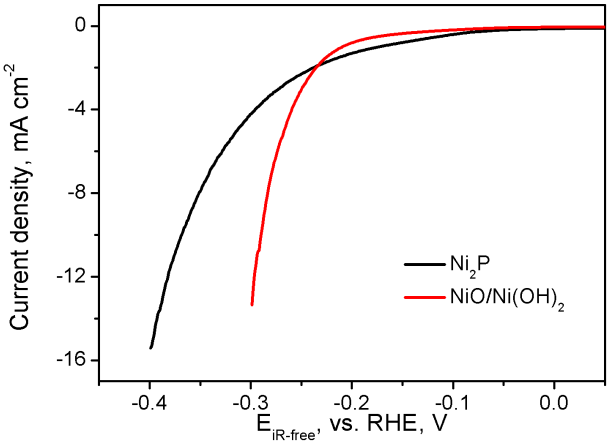

Fig. S4. Polarization curves of Ni_2P and $NiO/Ni(OH)_2$ electrodes in 0.1 M KOH electrolytes after 100 CV cycles.

ECSA of Ni_2P catalysts

Electrochemical active surface area (ECSA) of Ni_2P catalysts was estimated from their electric double layer capacitance (C_{dl}). Cyclic voltammetry (CV) scans of Ni_2P electrodes were recorded in a non-Faradic region (-0.035–0.035 V *vs.* reversible hydrogen electrode (RHE)) at the different scan rates (10, 20, 30, 40 and 50 mV s^{-1}) in 0.5 M H_2SO_4. Their anodic and cathodic current densities measured at the middle potential from CV scans were linearly fitted with the CV scan rates to obtain $Slope_{anodic}$ and $Slope_{cathodic}$, respectively.[2] C_{dl} was calculated by the equation (1):

$$C_{dl} = (Slope_{anodic} - Slope_{cathodic})/2 \quad (1)$$

ECSA was then calculated by dividing the C_{dl} using the specific surface capacitance (C_s) of the electrode surface:

$$ECSA = C_{dl} / C_s \quad (2)$$

Since the exact value of C_s for Ni_2P is not available, A commonly used C_s value (0.035 mF cm^{-2}) for metal surfaces was used in this study.[3-5]

C_{dl} of Ni_2P electrodes is ~0.285 mF, corresponding to the ECSA of 8.13 cm^2 for the electrode with the GSA of 0.5 cm^2. The much larger ECSA compared to GSA can be attributed to the rough surface of Ni_2P particles as shown in SEM images (Fig. 1b).

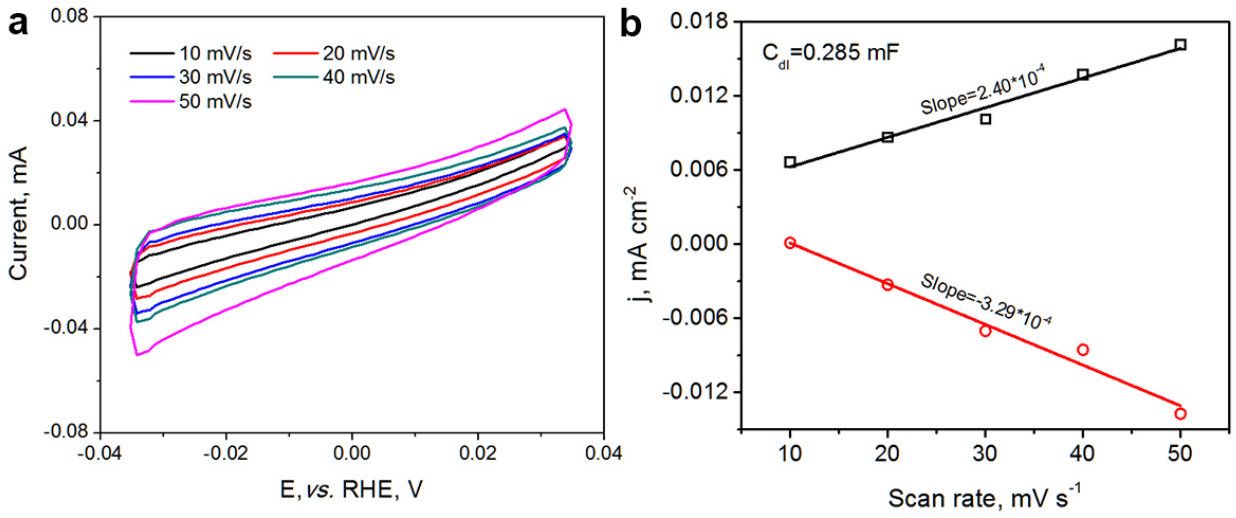

Fig. S5. (a) CV curves of the Ni_2P electrode at a non-faradic area in 0.5 M H_2SO_4 at the scan rates of 10, 20, 30, 40 and 50 mV s^{-1}. (b) Capacitive currents plotted as a function of the scan rate.

ECSA of Pt foil

ECSA of the Pt foil was determined from its CV curve in 0.5 M H_2SO_4 electrolyte at the scan rate of 50 mV s^{-1}. Three regions of current-potential response are included in the range from 0 to 1.6 V as shown in Fig. S7. First, the electro-adsorption and desorption of H_2 is located between 0.05 and 0.4 V with two redox peaks corresponding to strong and weak binding of H_2 at Pt (100) and (110) surfaces. Second, the double layer region has a constant current from 0.4 to 0.75 V. Third, an oxidation peak appears at E > 0.85 V in the positive-going scan and a reduced peak is observed around 0.8 V in the following negative-going scan. The redox peaks are caused by the formation and reduction of hydroxide/oxide on Pt. The amounts of charge exchanged during the electro-adsorption (Q') and desorption (Q'') of H_2 on Pt can be calculated using following equation:

$$Q = \frac{1}{v}\int_{E1}^{E2} I\,dE$$

where v is the scan rate. The blue region in Fig. S7 contributed by the capacitive current from the double layer capacitance is deducted from the total charge. The coulombic charge of H_2 desorption (Q_H) on Pt foil can be calculated from the equation:

$$Q_H = \frac{1}{2}(Q' + Q'')$$

ECSA of Pt foil was then calculated by the equation:

$$\text{ECSA} = \frac{Q_H}{0.21}$$

where the constant (0.21 mC cm^{-2}) represents the charge required to oxidize a monolayer of H_2 on Pt.[6] The charges Q_H, Q', Q'' and ECSA of Pt foil were summarized in Table S3.

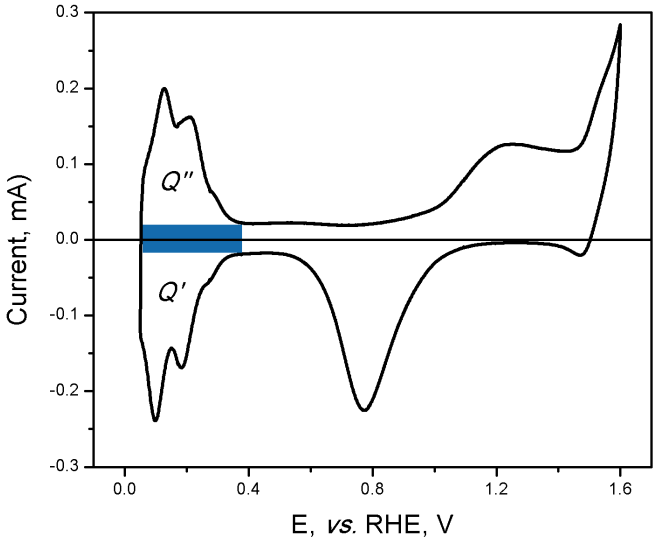

Fig. S6. ECSA calculation of Pt foil in 0.5 M H_2SO_4. The CV scan rate is 50 mV s^{-1}.

Table S4. Q_H, Q', Q'' and ECSA of Pt foil (2 cm^2)

Catalyst	Q' (mC)	Q'' (mC)	Q_H (mC)	ECSA (cm^2)
Pt foil	0.56	0.60	0.58	2.76

References cited in ESI:

1. W. Sheng, Z. Zhuang, M. Gao, J. Zheng, J. G. Chen and Y. Yan, *Nat. Commun.*, 2015, **6**, 5848.
2. Y. Yang, H. Fei, G. Ruan, C. Xiang and J. M. Tour, *ACS Nano*, 2014, **8**, 9518-9523.
3. B. Seo, D. S. Baek, Y. J. Sa and S. H. Joo, *CrystEngComm*, 2016, **18**, 6083-6089.
4. C. C. McCrory, S. Jung, J. C. Peters and T. F. Jaramillo, *J. Am. Chem. Soc.*, 2013, **135**, 16977-16987.
5. C. C. McCrory, S. Jung, I. M. Ferrer, S. M. Chatman, J. C. Peters and T. F. Jaramillo, *J. Am. Chem. Soc.*, 2015, **137**, 4347-4357.
6. A. Pozio, M. De Francesco, A. Cemmi, F. Cardellini and L. Giorgi, *J. Power Sources*, 2002, **105**, 13-19.